

\*\*FULL TITLE\*\*  
*ASP Conference Series, Vol. \*\*VOLUME\*\**, © \*\*YEAR OF PUBLICATION\*\*  
 \*\*NAMES OF EDITORS\*\*

## Tracking Evolutionary Processes with Large Samples of Galaxy Pairs

Elizabeth J. Barton, Christopher Q. Trinh, James S. Bullock, and Shelley A. Wright<sup>1</sup>

*Center for Cosmology, University of California, Irvine*

**Abstract.** Modern redshift surveys enable the identification of large samples of galaxies in pairs, taken from many different environments. Meanwhile, cosmological simulations allow a detailed understanding of the statistical properties of the selected pair samples. Using these tools in tandem leads to a quantitative understanding of the effects of galaxy-galaxy interactions and, separately, the effects quenching processes in the environments of even very small groups. In the era of the next generation of large telescopes, detailed studies of interactions will be enabled to much higher redshifts.

### 1 Introduction

In many ways, the early stages of galaxy-galaxy interactions are the easiest to identify and study. When they exist as a resolved pair, large samples of hundreds or thousands of pre-merger galaxies can be selected readily and objectively from a redshift survey (e.g., Barton et al. 2000; Lambas et al. 2003; Nikolic et al. 2004). This technique has a major advantage: subjective, morphological, and/or kinematic measures of whether two galaxies are merging are completely unnecessary. Because the common indicators of interaction depend on merger stage and surface brightness, and because they can miss retrograde encounters and minor interactions, samples selected based on merger signatures are less complete than pair samples.

Unfortunately, pair samples include significant contamination from pairs that are physically well separated and seen projected, pairs that are not physically close but are part of the same larger group, and pairs that have not yet interacted. In Barton et al. (2007), we use cosmological  $N$ -body simulation coupled with a semianalytic substructure model (Zentner & Bullock 2003; Zentner et al. 2005) to explore the contamination inherent in pair samples selected from redshift surveys. Here, we describe that technique and extend it to study star formation suppression in small groups.

### 2 Close Pairs and Triggered Star Formation

Barton et al. (2007) contains a detailed description of our technique for isolating triggered star formation in galaxy pairs. The essence of the approach is to

---

<sup>1</sup> Present Affiliation: University of California, Berkeley

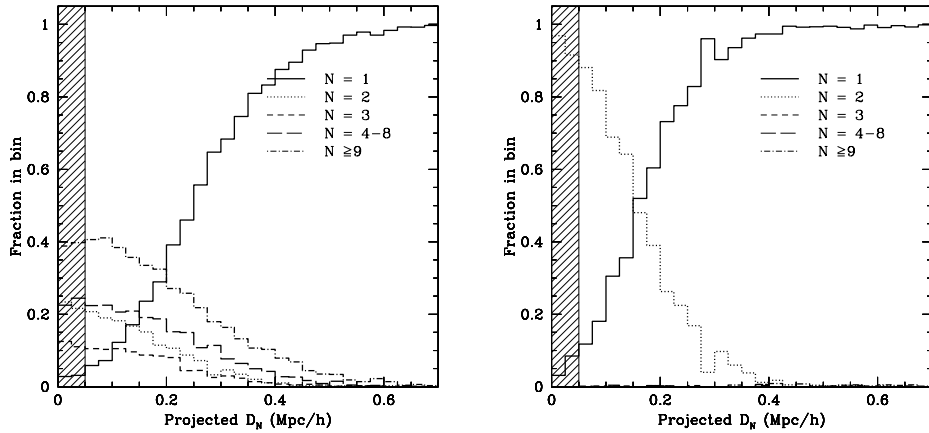


Figure 1. Properties of pairs in a cosmological simulation, from Barton et al. (2007). Using a cutoff halo maximum velocity of  $160.5 \text{ km s}^{-1}$ , we bin the data by the projected distance to the nearest neighbor,  $D_N$ , within  $1000 \text{ km}^{-1}$  and plot the fraction of galaxies in each bin with a given of the number of massive subhalos,  $N$  (including the central galaxy). We plot the full sample (*Left*) and the sample with at most one neighbor within  $700 \text{ h}^{-1} \text{ kpc}$  (*Right*). If no isolation criteria are applied, apparent pairs are *mostly* galaxies in larger groups typically with  $\geq 4$  members. If the isolation criterion is applied, close pairs are primarily isolated  $N = 2$  systems.

identify galaxy pairs that are unlikely to be part of larger and more complex systems, to estimate the likely contamination from isolated galaxies seen in projection, and to identify an appropriate control sample of isolated galaxies for direct comparison. We use the cosmological model to understand galaxies in pairs. Specifically, we create an artificial volume-limited redshift survey from the hybrid  $N$ -body simulation and substructure model by matching the abundances of simulated dark matter halos and sub-halos to the abundances of the galaxies in the redshift survey. This technique rests only on the assumption that galaxy luminosity depends monotonically on halo mass or, in our case, on the surrogate maximum circular speed of the simulated halo or sub-halo,  $V_{\max}$ . For sub-halos, we use the circular speed of the dark matter halo at the time it fell into the parent halo because it is consistent with the two-point correlation function and pair counts statistics of existing redshift surveys (Conroy et al. 2006; Berrier et al. 2006).

Fig. 1a employs this technique, showing the primary limitation of pair samples selected from redshift surveys. For a volume-limited sample that corresponds to  $M_{B,j} \leq -19$  in the 2dF Galaxy Redshift Survey (Colless et al. 2001), we show that most galaxies in close pairs are actually members of larger groups of 3 or more galaxies. As a result, many galaxies in statistical pair samples are actually cluster or group galaxies, which likely have suppressed star formation for other reasons. This effect causes a strong and systematic underestimate of the aggregate amount of star formation in close galaxy-galaxy pairs. This effect, and not dust, is likely responsible for the result that somewhat widely separated

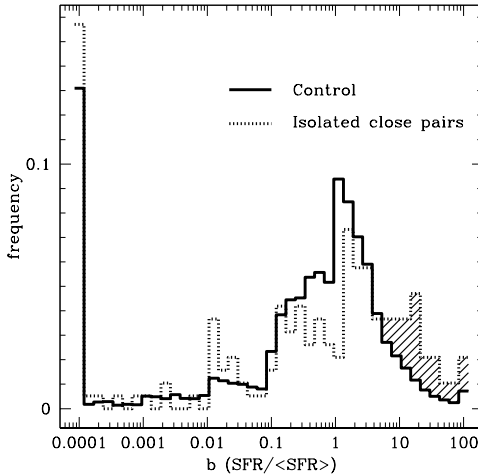


Figure 2. A fair comparison of isolated galaxies (*Solid line*) and isolated close pairs (*Dashed line*), from Barton et al. (2007). We plot histograms of the star formation rate divided by the average past star formation rate, as estimated from the 2dF spectra (see Colless et al. 2001; Madgwick et al. 2003; Barton et al. 2007), for the isolated galaxies and the isolated pairs. The isolated pairs show a significant (14%) excess of star-forming galaxies with rates boosted by  $b \geq 5$  (*Shaded histogram*).

pairs ( $\sim 60\text{-}100 \text{ h}^{-1} \text{ kpc}$ ) are actually *redder* than the field (e.g., Sol Alonso et al. 2006).

If we restrict the sample to galaxies with at most one neighbor within  $700 \text{ h}^{-1} \text{ kpc}$  on the sky and  $1000 \text{ km s}^{-1}$  in redshift, however, as we do in Fig. 1b, it becomes straightforward to identify isolated galaxy pairs. For pairs with separations  $\leq 50 \text{ h}^{-1} \text{ kpc}$ , the contamination in the pair sample from isolated ( $N = 1$ ) galaxies is  $\leq 10\%$  and the contamination from systems with  $\geq 3$  members is negligible.

In Fig. 2, we show the distribution of star-forming properties of isolated galaxies and isolated pairs measured via this technique from the 2dF survey (Colless et al. 2001). The close ( $\leq 50 \text{ h}^{-1} \text{ kpc}$ ) pairs show a distinct, 14% excess of galaxies with high star formation rates. In Barton et al. (2007), we show that the ability to measure this effect accurately depends dramatically on whether pairs in denser environments are removed from the sample.

### 3 Widely Separated Pairs and the Evidence for Quenching and “Strangulation”

While close pairs are ideal for the study of triggered star formation, more widely separated isolated pairs reveal other group processes. Most galaxies in systems with  $N = 2$  members have actually not had a recent close galaxy-galaxy pass. In Fig. 3, we use the simulation to compute the cumulative number of galaxies that have had a close pass “recently” (200 Myr to 1 Gyr ago), for two different halo masses (or  $V_{\text{max}}$  values), corresponding to two different magnitude limits

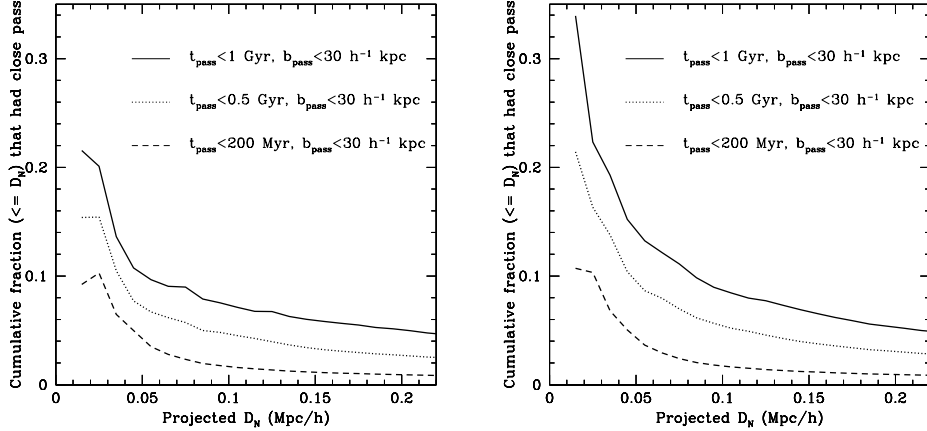


Figure 3. The cumulative fraction of isolated pairs that have had a close ( $\leq 30 \text{ h}^{-1} \text{ kpc}$ ) pass recently, where “recently” is either 1 Gyr (Solid line), 500 Myr (Dotted line), or 200 Myr (Dashed line), as a function of the distance to the nearest neighbor. We plot the fraction for two different cutoffs, including (Left) all halos with  $V_{\text{max}} \geq 160.5 \text{ h}^{-1} \text{ kpc}$ , appropriate for comparison to the 2dF work in Barton et al. (2007), and (Right) with  $V_{\text{max}} \geq 140 \text{ h}^{-1} \text{ kpc}$ , appropriate for comparison to a volume limited SDSS sample with  $M_r + 5 \log h \leq -19$  (e.g., Trinh et al. 2009). The fraction of pairs that have had close passes recently is a strong function of  $D_N$ .

for the data. In both cases, the fraction of galaxies that have had a close pass is a strong function of the distance to their nearest neighbor, becoming  $\leq 10\%$  for pair samples with maximum separations above  $D_N \sim 0.1 \text{ h}^{-1} \text{ Mpc}$ . As a result, more widely separated pair samples can be used to study whether the processes that cause the morphology-density relation (e.g., Dressler 1980; Postman & Geller 1984) operate in extremely sparse systems that have only two members. These processes include rapid quenching, where the cold gas is stripped directly from the system, and “strangulation,” where only the rarefied outer halo is removed.

In Fig. 4, we demonstrate the difference in color distributions between the wider pairs and isolated galaxies of the same stellar mass. The satellite galaxy is defined as the less luminous member of each pair ( $r$ -band). The satellites show a slight blue excess, presumably due to triggered star formation, and a much stronger red excess due to quenching and/or “strangulation.” Specifically, 21% more satellites than isolated galaxies are redder than  $g - r = 0.68$ , *even when galaxies with the same stellar masses are compared*. Thus, 21% of satellite galaxies in even the tiny  $N = 2$  systems have moved from the blue to the red sequence. At least some of the processes that give rise to the morphology-density relation operate in even very sparse groups.

The right side of Fig. 4 uses the simulation to measure the amount of time that the satellites (subhalos) have been substructure in these  $N = 2$  systems. Almost independent of star formation history, it takes roughly 2 Gyr to go from blue to red when star formation stops. If star formation ceased as soon as the galaxy became substructure, roughly  $\sim 60\%$  of all satellites would have stopped

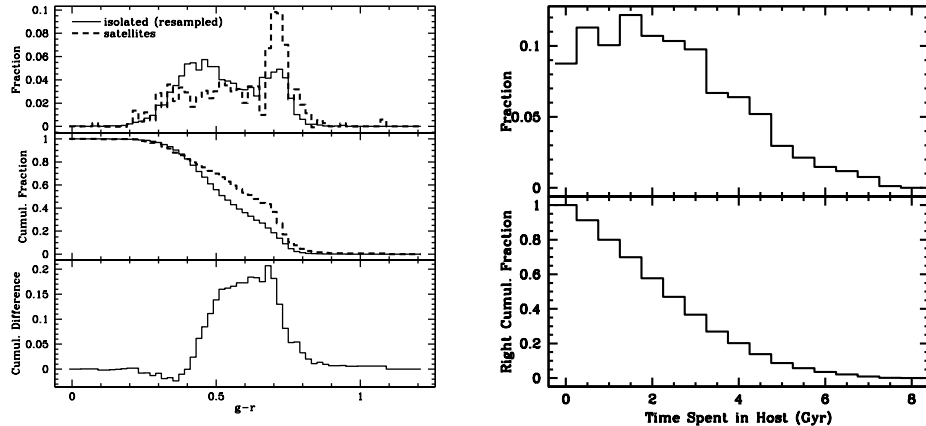


Figure 4. Widely separated pairs from the SDSS, adapted from Trinh et al. (2009). (Left) We plot histograms of  $g-r$  color for isolated galaxies and satellite galaxies in pairs with  $D_N \leq 200 \text{ h}^{-1} \text{ kpc}$  (Top), along with the cumulative distributions (Middle) and the difference between the cumulative distributions (Bottom). The pairs have had contamination from isolated galaxies subtracted and the isolated galaxies have been resampled to the same stellar mass distribution as the satellites. (Right) From the simulations, we plot the differential (Top) and cumulative (Bottom) distributions of the amount of time that subhalos of  $N = 2$  systems have spent as substructure.

forming stars. Because  $\sim 77\%$  were blue to begin with, roughly  $\sim 46\%$  of the satellites would have moved from blue to red. Because the number that have actually moved from blue to red is only 21%, we conclude that star formation continues well after a galaxy becomes substructure, for typically  $\sim 2$  Gyr. This analysis yields significant constraints on quenching and ram pressure stripping outside of the cluster environment (Trinh et al. 2009).

#### 4 Detailed Studies at High Redshift: the Next Generation of Large Ground-based Telescopes

With present-day technology, the signatures of interaction are difficult to identify unambiguously at high redshift. New kinematic techniques enabled by adaptive optics and integral field unit spectrographs are effective (e.g., Wright et al. 2009; Förster Schreiber et al. 2009). However, these observations are limited to the brightest systems and do not reveal individual star-forming clusters. In the era of the next generation of large optical and infrared telescopes, adaptive optics and huge mirror sizes will allow a very detailed identification of merging systems. In Fig. 5, we present a simulation of the Antennae galaxies observed with the Thirty Meter Telescope (TMT) and the InfraRed Imaging Spectrograph (IRIS), which is planned to work with adaptive optics at first light. The observation reveals individual superstar clusters even at  $z \sim 3$ , and likely beyond, allowing very detailed kinematic and metallicity maps of the galaxy.

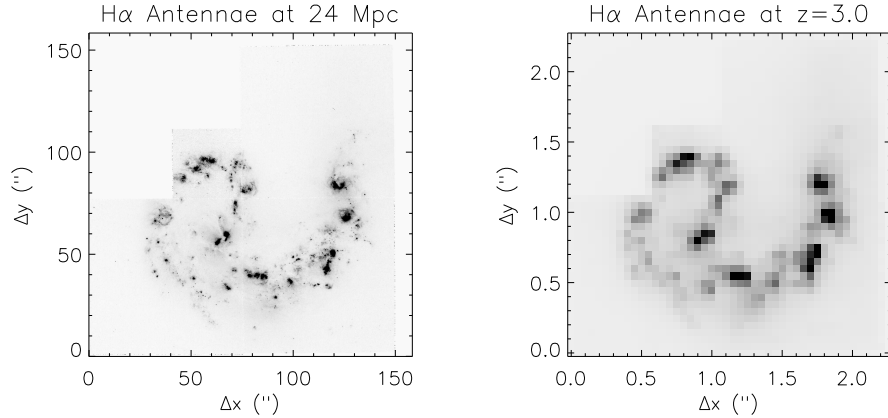


Figure 5. A simulation of the Antennae observed at  $z = 3$ . We show an  $\text{H}\alpha$  image of the Antennae courtesy of B. Whitmore (*Left*) and a simulation artificially redshifted to  $z \sim 3$  and observed with the an integral field unit spectrograph on the Thirty Meter Telescope (*Right*) with an exposure time of 3 hours and a sampling of 50 mas. Individual star-forming lumps are discernible with TMT and will yield an accurate kinematic map of the system.

**Acknowledgments.** We would like to thank our collaborators, Risa H. Wechsler and Andrew R. Zentner, for allowing us to quote these results prior to publication. We would also like to thank Brad Whitmore for sharing his reduced  $\text{H}\alpha$  image of the Antennae.

## References

Alonso, M. S., Lambas, D. G., Tissera, P., & Coldwell, G. 2006, MNRAS, 367, 1029  
 Barton, E. J., Geller, M. J., & Kenyon, S. J. 2000, ApJ, 530, 660  
 Barton, E. J., Arnold, J. A., Zentner, A. R., Bullock, J. S., & Wechsler, R. H. 2007, ApJ, 671, 1538  
 Berrier, J. C., Bullock, J. S., Barton, E. J., Guenther, H. D., Zentner, A. R., & Wechsler, R. H. 2006, ApJ, 652, 56  
 Colless, M., et al. 2001, MNRAS, 328, 1039  
 Conroy, C., Wechsler, R. H., & Kravtsov, A. V. 2006, ApJ, 647, 201  
 Dressler, A. 1980, ApJ, 236, 351  
 Förster Schreiber, N. M., et al. 2009, arXiv:0903.1872  
 Lambas, D. G., Tissera, P. B., Alonso, M. S., & Coldwell, G. 2003, MNRAS, 346, 1189  
 Madgwick, D. S., Somerville, R., Lahav, O., & Ellis, R. 2003, MNRAS, 343, 871  
 Nikolic, B., Cullen, H., & Alexander, P. 2004, MNRAS, 355, 874  
 Postman, M., & Geller, M. J. 1984, ApJ, 281, 95  
 Trinh, C. Q., Barton, E. J., Bullock, J. S., Zentner, A. R., & Wechsler, R. H. 2009, in prep.  
 Wright, S. A., Larkin, J. E., Law, D. R., Steidel, C. C., Shapley, A. E., & Erb, D. K. 2009, ApJ, 699, 421  
 Zentner, A. R., & Bullock, J. S. 2003, ApJ, 598, 49  
 Zentner, A. R., Berlind, A. A., Bullock, J. S., Kravtsov, A. V., & Wechsler, R. H. 2005, ApJ, 624, 505